Int. J. Electrochem. Sci., 15 (**2020**) 5277 – 5286, doi: 10.20964/2020.06.41

International Journal of
ELECTROCHEMICAL
SCIENCE
www.electrochemsci.org

Short Communication

Failure Behavior of Nickel Silicide Diffusion Barrier between Electroplating Cu and Textured Si Substrate

Hsin Hsan Wu[1] *and Wen Jauh Chen*[2,*]

[1] Department of Mechanical Engineering, National Yunlin University of Science and Technology, Douliu, Yunlin, Taiwan.
[2] Graduate School of Materials Science, National Yunlin University of Science and Technology, Douliu, Yunlin, Taiwan.
[*]E-mail: chenwjau@yuntech.edu.tw

Received: 17 January 2020 / *Accepted:* 7 March 2020 / *Published:* 10 May 2020

Copper metallization has the potential to introduce into solar cell front side contact instead of screen printing. However, copper can react with silicon to form copper silicide quickly. A diffusion barrier needs to be introduced to avoid copper diffusion into the silicon substrate. Nickel silicide has been as the diffusion barrier in solar cells. The nickel silicide barrier layer also increases the adhesion strength of plated Ni/Cu. In this work, the nickel silicide barrier layer formed by electroless nickel plating method. And the degradation of the nickel silicide barrier layer in structure Cu/$NiSi_x$/Si will be investigated. The structures of Cu/$NiSi_x$/Si characterized by scanning electron microscopy (SEM), scanning transmission electron microscope (STEM), energy dispersive X-ray spectrometer (EDS), and powder X-ray diffraction (XRD). The results show that the failure of Cu/$NiSi_x$/Si can be attributed to copper react with nickel silicide to form Cu-Ni-Si alloy first. Then the copper penetration through the thin nickel silicide layer and the formation of copper silicide.

Keywords: Textured silicon; Nickel silicide; Solar cells; Diffusion barrier

1. INTRODUCTION

At present, screen printed silver paste is the current method for front side metallization of crystalline Si solar cells in the photovoltaic industry. The strong points of screen-printing are a natural process, low fabrication, and quick metal deposition process [1, 2]. Screen printed silver paste requires an 800 °C firing process to form a metal contact on the silicon. As a result of the high-temperature process, the performance losses. Besides, the front silver metallization cost is the most considerable individual cost fraction in the costs of solar cell production [3-5]. The price of copper is about 100 times cheaper than silver. And copper has high conductivity. There is a great potential to reduce the production

costs of silicon solar cells significantly by substitution of the silver with copper. In general, the front side copper metallization process is based on the light-enhanced deposition. The light-enhanced deposition includes light-induced electrolytic nickel deposition and light-induced copper deposition [6].

The electroplating copper technology can be applied to the front metallization of solar cells. Although it can overcome the shortcomings of the screen printing, however, copper has high mobility in silicon and as a highly active recombination center in solar cells [7-9]. To prevent copper penetration into the silicon substrate and avoid the formation of copper silicide. A diffusion-inhibiting intermediate layer between the copper layer and the silicon substrate will be introduced, and prevent direct contact between copper and the bottom Si. Till now, a nickel layer, nickel silicide, and nickel-cobalt alloy as the diffusion barrier in solar cells have been studied [10-14]. The nickel silicide barrier layer also increases the adhesion strength of plated Ni/Cu [15].

Recently, Kale et al. reported enhancing the degradation of the NiSi film attributed to Cu combined with the high-temperature annealing [10]. Kale et al. also investigated the thermal stability of Cu contacts with both Ni and NiSi barrier layers using a single-side-polished silicon substrate. They identified interfacial reactions responsible for the degradation of both Ni and NiSi layers. Their results have shown that the Cu/NiSi/Si contact is a much more thermally stable, and a better diffusion barrier to Cu than the Cu/Ni/Si contact [11]. The presence of Cu deteriorates the barrier properties of NiSi film by slowly dissolving it at elevated temperatures. We also show that a thicker NiSi film is thermally more stable while mitigating Cu diffusion. Huang et al. prepared solar cell using CMOS (complementary metal-oxide-semiconductor) grade and without textured (100) silicon as a substrate. In their report showing that the single Ni_2Si layer cannot prevent copper diffusion into silicon. And the Ni/Ni_2Si double-layer delays the degradation at 200 ℃ [12]. Our previous study also found that the copper diffused into silicon and formed Cu_3Si after annealing at 300 ℃ for 10 min in the Cu/Ni (60 nm)/NiSi/Si system [13]. The detail failure of the nickel silicide barrier does not report in the literature. In this study, the failure of the nickel silicide barrier layer was studied by STEM.

2. EXPERIMENTAL

The substrate used in this study is a single crystal phosphorus-doped pyramid textured silicon wafers. The textured silicon substrate surface degreases in acetone by ultrasonic and using H_2SO_4/H_2O_2 solution first. Then textured silicon substrate is dipping into hydrogen fluoride (HF) solution to obtain the fresh surface of textured silicon. The electroless nickel film is deposited on the textured silicon. To plate nickel film on silicon by the electroless method. The sensitization and activation of silicon are necessary. A solution of sensitization comprises of $SnCl_2$ and HCl, and activation solution consists of $PdCl_2$ and HCl. After sensitization and activation, the electroless nickel film can be plated onto the textured silicon. In this study, the electroless plating bath with a pH value of 5 and a temperature of 70 °C was used to plate nickel film. The plating time was 60 seconds.

To the formation of nickel silicides, the substrate with thin nickel film was first annealed in a furnace at 500 °C in Ar/H_2 atmosphere for 10 minutes. The nickel silicides formed on the silicon substrate after 500 °C annealing. To obtain the clean surface of the annealing sample, the unreacted

nickel-metal removed by the HNO_3 solution to form the structure of $NiSi_x$/Si. The clean $NiSi_x$/Si substrate was used to further electroplating copper films. The dimension of substrates was set at 20 mm x 20 mm. The process of electroplating copper on $NiSi_x$/Si substrates is conducted on chemical baths. The electroplating bath is operated at a temperature of 25 °C. The anode material uses the platinum plate with a size of 20 mm x 20 mm. The electroplating time of the copper layer is about 4 minutes. The preparation of chemical baths solution used the reagent grade chemicals and deionized water. A beaker of 300 mL was used as an electroplating cell. The magnetic stirrer agitation was applied during electroplating. The electroplating copper metals on $NiSi_x$/Si are designed as Cu/$NiSi_x$/Si. Finally, the Cu/$NiSi_x$/Si samples were annealed at 300 - 800 °C for 10 min in Ar/H_2 ambient.

A JEOL scanning electron microscopy (SEM) operating at 20 kV was used for surface morphologies examination. A scanning transmission electron microscope (STEM) was performed on a JEM-ARM200F. An SEM that has an energy dispersive X-ray spectrum (EDS, Oxford Link), which we used to determine the chemical composition of all samples. The STEM-EDS compositional maps were also using an EDS detector (JEOL Ltd.) to collect x-rays. Powder X-ray diffraction (XRD) analyses were performed on a Bruker D8 Advance diffractometer with Cu Kα radiation.

3. RESULTS AND DISCUSSION

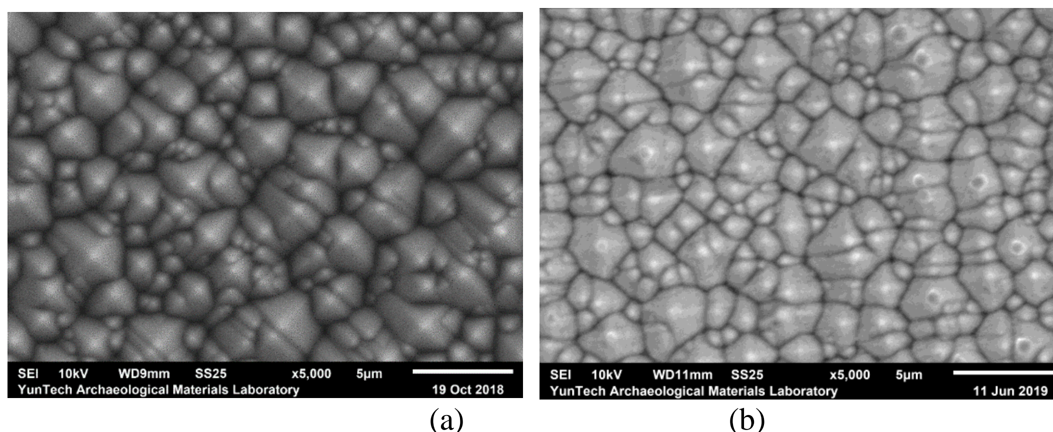

Figure 1. (a) presents an SEM micrograph for the surface structure of original textured single crystal silicon. (b) SEM micrograph for the surface structure of plated nickel film and annealed sample.

Figure 1 (a) presents an SEM micrograph for the surface structure of original textured single crystal silicon. Many pyramid shapes exist on the surface of the single-crystal silicon substrate. The surface structure of the sample that thin electroless nickel film was deposited onto the substrate and annealed in a furnace at 500 °C in Ar/H_2 atmosphere for 10 min shown in figure 1 (b). It is a layer of nickel silicide on the surface from the SEM image.

Figure 2 (a) is a STEM micrograph that shows the layer structure of the as-deposited sample of Cu/NiSi/Si. STEM–EDS can provide elemental maps as a powerful method to locate all layers. The EDS

maps of Cu, Ni, and Si are shown in Fig. 2 (b)-(d), respectively. EDS maps of Fig. 2 (b)-(d) use the Cu K, Ni K, and Si K lines. The EDS elemental maps show three distinct layers.

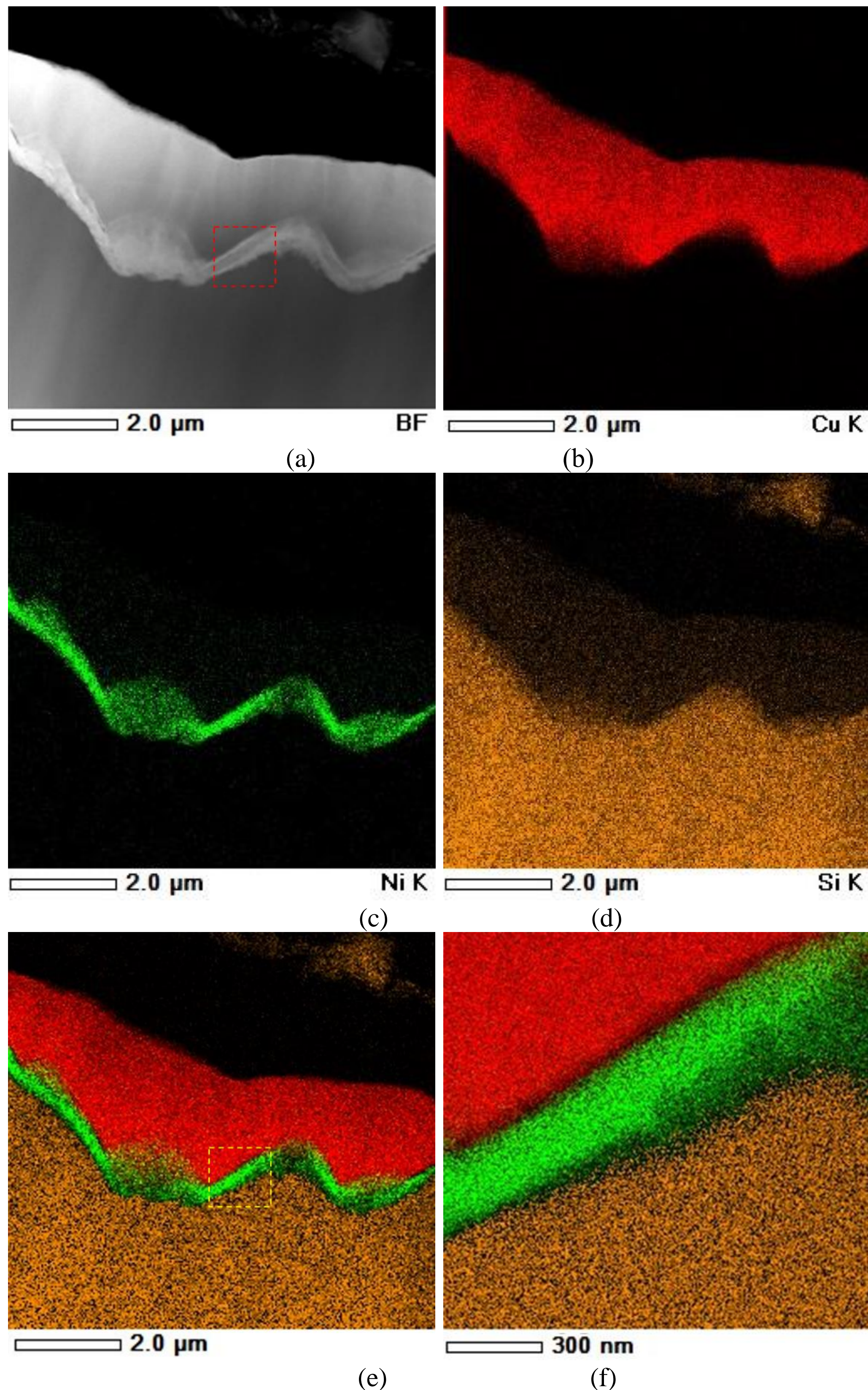

Figure 2. (a) STEM bright-field image of Cu/Ni/Si as-deposited sample, EDS map of (b) Cu, (c) Ni, (d) Si, and (e) an overlay of Cu, Ni, and Si EDS map, and (f) an enlarge image of (e).

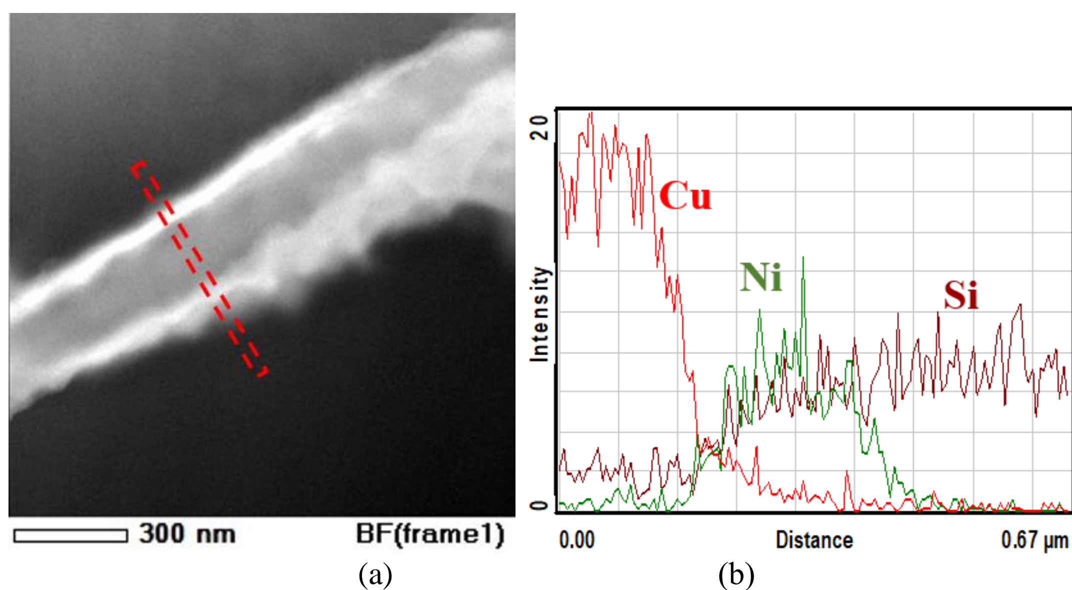

(a) (b)

Figure 3. (a) STEM bright-field image of Cu/Ni/Si as-deposited sample. (b) the composition analysis was carried out across the stack using STEM-EDS.

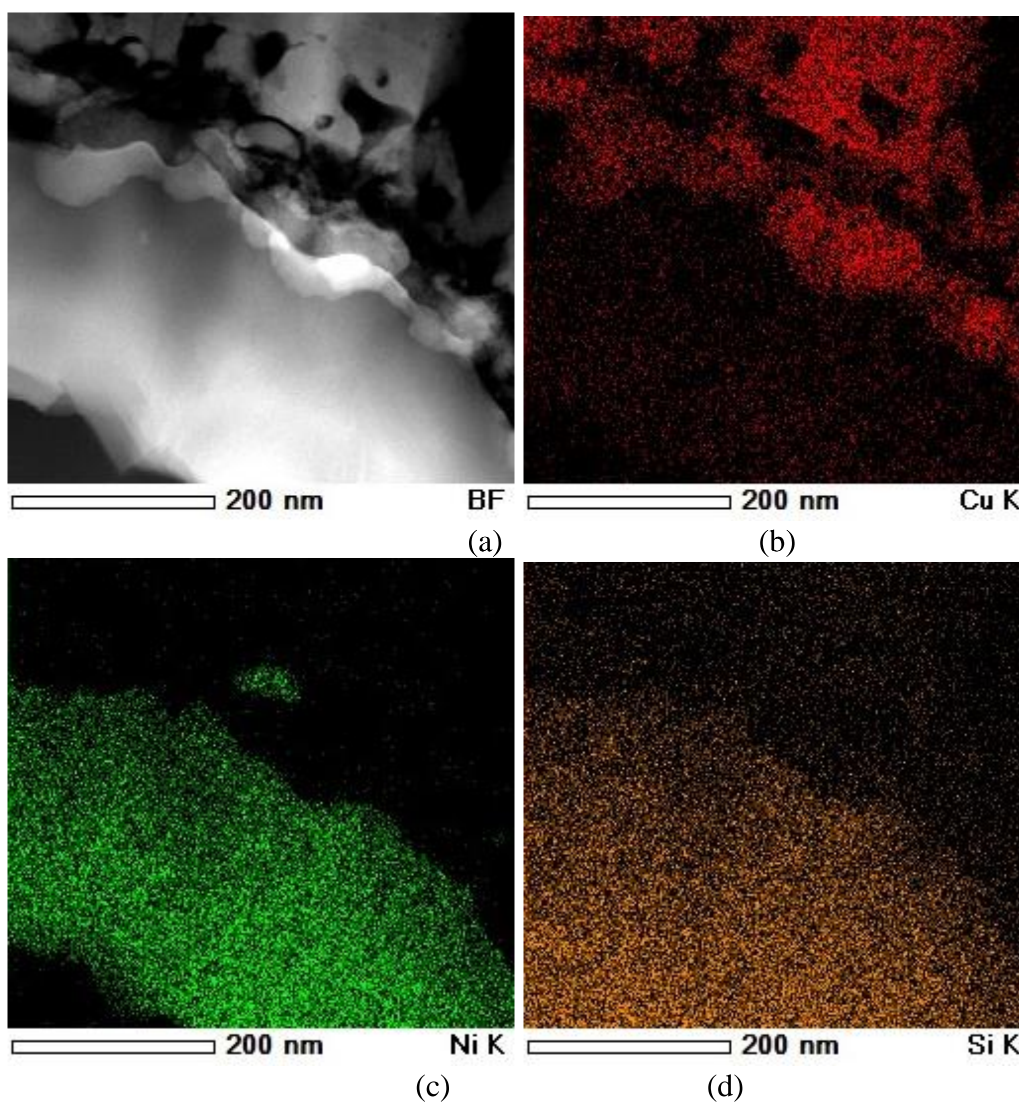

(a) (b)

(c) (d)

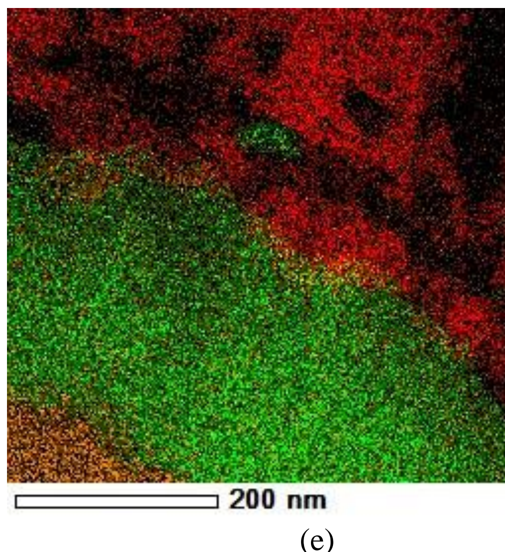

(e)

Figure 4. (a) STEM bright-field image of the sample annealed at 300 °C, EDS map of (b) Cu, (c) Ni, (d) Si, and (e) an overlay of Cu, Ni, and Si EDS map.

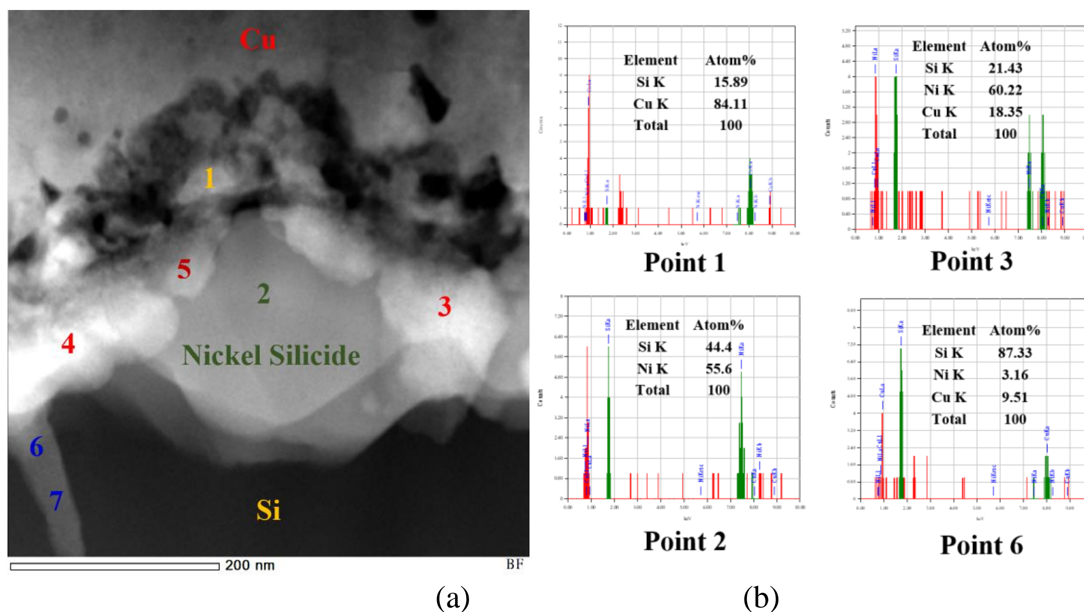

(a) (b)

Figure 5. (a) STEM bright-field image of the sample annealed at 300 °C, (b) Spot elemental analysis of points 1, 2, 3, and 6.

The uniform intensity of layer 1 (top layer, Fig. 2(b)) area shows that it is constituted of Cu without Ni and Si. Layer 2 (Fig. 2(c)) is a Ni element map. Fig. 2 (d) shows the Si spectra that can be easily identified as belonging to the chemical phases of Si. The nickel layer is overlapped with part of the silicon layer from the figure (c) and (d), which reveals the Ni layer is nickel silicide. Fig. 2(e) shows an overlap of Cu, Ni, and Si maps, and the overlap area of Ni and Si are constituted of Ni and Si. Fig. 2 (f) shows an enlarged image of the rectangle area of figure 2 (a) and (f). The thickness of the nickel silicide (Ni+Si) layer was measured to about 250 nm. STEM-EDS line scanning allowed us to find the profile of element in the multilayer structure. The composition analysis was carried out across the stack

using STEM-EDS, present in figure 3. Fig. 3 (b) shows the compositional profile of the rectangle area, which shows in figure 3 (a). The distribution of copper in the stack was found to concentrate on the left side. This finding suggested that copper did not diffuse into the silicon substrate. The distribution of nickel in the stack was found to focus on the middle area. The distribution of silicon in the stack was found to concentrate on the central region and right side. The intensities of signal nickel and silicon in the middle area are almost the same. This finding suggested that the nickel silicide layer reveals the presence of NiSi.

Figure 4 (a) is a STEM bright-field image of Cu/NiSi/Si sample annealed at 300 °C. Some compounds were found in the interface between nickel silicide and copper. To understand the chemical compositions of the compounds. The EDS maps of Cu, Ni, and Si are shown in Fig. 4 (b)-(d), respectively. The copper layer is overlapped with part of the nickel silicide layer from the figure (b) and (c). Which reveals the compound in the interface comes from the reaction of the copper layer and nickel silicide layer. Fig. 4(e) shows an overlap of Cu, Ni, and Si maps, and the compound is constituted of Cu, Ni, and Si.

Fig. 5 shows the spot elemental analysis of the same sample but a different area. The compound near the copper layer is constituted of Cu and Si, which reveals the Si element in NiSi film has reacted with the Cu and form the copper silicide. Points 2 indicated the nickel silicide layer without copper. Which explains thick nickel silicide layer can prevent the diffusion of copper. There is a copper element has found on the nickel silicide layer from point 3. The composition (atomic percent) of the point 4 and 5 are about Si(58%)-Ni(27%)-Cu(15%) and Si (57%)-Ni(23%)-Cu(20%), respectively. This reveals the copper has distributed through the thin nickel silicide layer when NiSi surface in contact with Cu at a temperature of 300 °C. Kale et al. also conclude that the NiSi surface in contact with Cu starts to dissolve forming Cu_3Si at 450 °C from XRD analysis [11]. Kale et al. also found the degradation of NiSi is slow, and the integrity of the NiSi layer for preventing Cu diffusion can be prolonged by using a thicker NiSi film at annealing temperatures ≤ 200 °C [11]. Zhao et al. also presented thermal stability of Cu/NiSi (80 nm)/Si stack [16]. Their result shows after annealing at 400 °C there was no detectable Cu_3Si phase and formation of Cu_3Si after annealing at 500 °C. A small amount of Cu_3Si hard to detect by using the XRD technique. Therefore, Zhao and Kale et al. found Cu_3Si at a higher temperature. A small amount of Cu_3Si can be found by the STEM technique. Point 6 and 7 have composition with Si(87%)-Ni(3%)-Cu(9%) and Si (91%)-Cu(9%), respectively. This suggests copper has diffused through the thin nickel silicide layer and formation of copper silicide in the silicon substrate. Based on these results, we can evidence that Cu dissolves in the nickel silicide first. Then the formation of copper silicide in the silicon substrate when the nickel silicide layer is thin enough. A similar phenomenon was also reported by Abhijit S. Kale et al. [11]. The sputtering vacuum process was applied to prepare thin nickel film and form the NiSi/Si system in the reports of Zhao and Kale et al. The thin nickel film made by the electroless method and develop NiSi after annealing in this study. The copper film is also prepared by electroplating. Therefore, the properties of NiSi formed by the electroless method may be different from the NiSi formed by the vacuum method.

XRD analyses were carried out to obtain more information about the phase formation during the annealings. XRD spectra for the samples annealed at 300–800 °C are presented in Fig. 6. XRD analysis shows almost exactly the same pattern for all annealing samples except for some changes in relative

intensities. Based on these XRD spectra, a small amount of copper silicide (Cu_3Si) was found annealed at 300°C. The strong intensity of Cu_3Si peaks is presented at a temperature higher than 600°C. XRD analyses are in agreement with the results of STEM. STEM bright-field micrograph of Cu/NiSi/Si sample annealed at 700 °C is presented in figure 7. The nickel silicide located at the top of the multilayer after annealing at 700 °C for 10 min. And the nickel silicide layer became a discontinuous film. STEM micrograph reveals that the little agglomeration and voids formation of nickel silicon films has taken place. Fig. 7 (b)-(d) shows the EDS maps of Cu, Ni, and Si, respectively. Fig. 7 (e) shows the overlap of Cu, Ni, and Si maps. The elemental maps reveal the Cu element is present in the nickel silicide layer and the upside of the silicon substrate, which shows that copper silicide exists between the nickel silicide layer and the silicon substrate. The results of STEM evidence that copper is diffused through the nickel silicide layer to the silicon substrate and reacted with silicon to form a copper silicide.

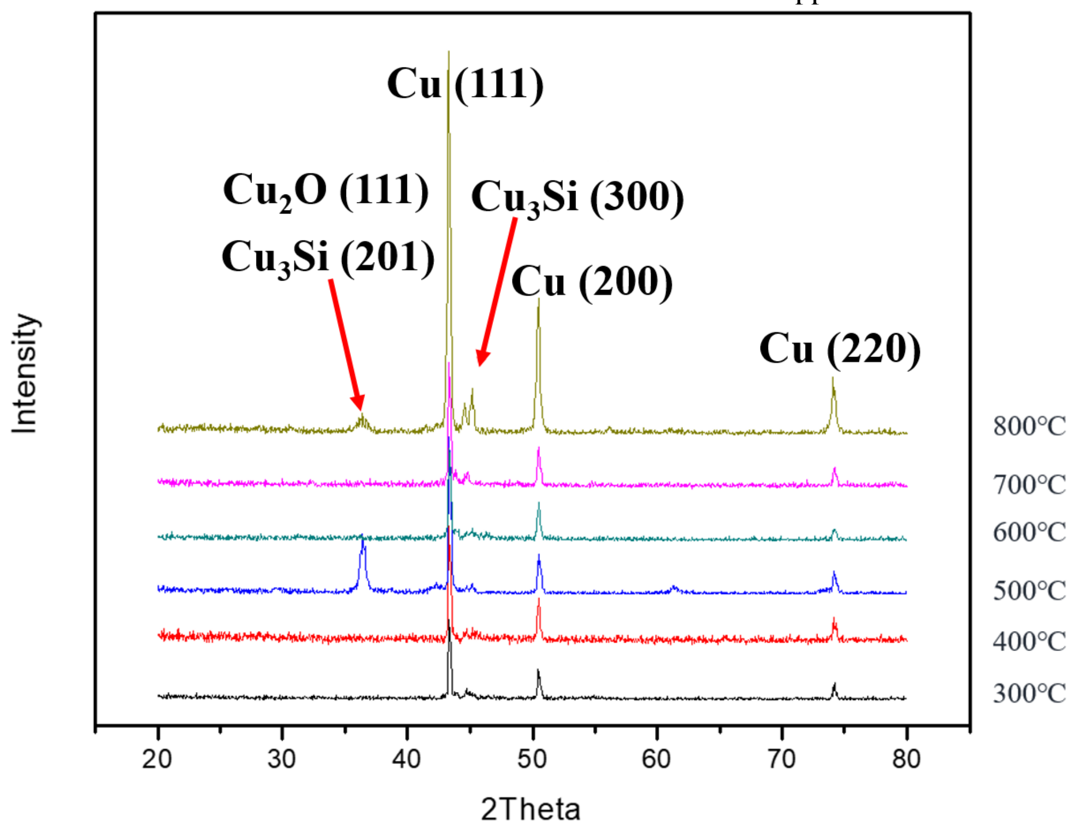

Figure 6. X-ray diffraction patterns of Cu/NiSi/Si samples annealed at various temperatures (300–800℃) for 10 min.

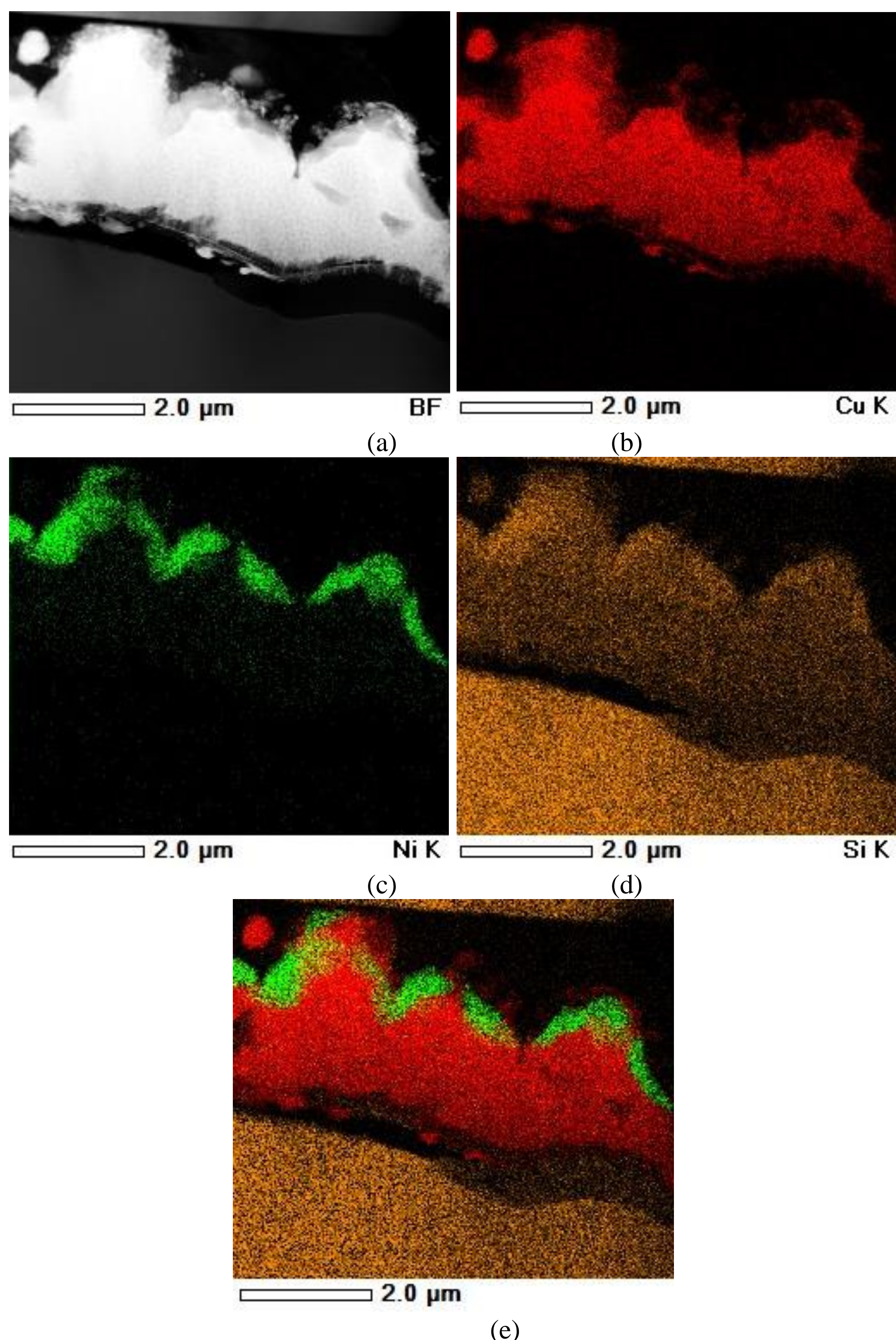

Figure 7. (a) STEM bright-field image of the sample annealed at 700 °C, EDS map of (b) Cu, (c) Ni, (d) Si, and (e) an overlay of Cu, Ni, and Si EDS map.

4. CONCLUSIONS

We have investigated the nickel silicide diffusion barrier performance for copper metallization. The formation of Cu-Ni-Si and Cu-Si alloy has found in the interfacial between copper and nickel

silicides in the Cu/$NiSi_x$/Si structure after annealing at 300 °C for 10 min. The Cu-Ni-Si alloy was found on the top of the nickel silicide layer when the nickel silicide layer is thick enough. However, the copper has distributed through the nickel silicide layer when the nickel silicide is very thin. This suggests copper has diffused through the thin nickel silicide layer and formation of copper silicide in the silicon substrate. Based on these results, we can evidence that Cu dissolves in the nickel silicide first. Then the formation of copper silicide in the silicon substrate when the nickel silicide layer is thin enough.

ACKNOWLEDGMENTS
Authors would like to thank Mr. Koichi Higashimine at the Center for Nano Materials and Technology, Japan Advanced Institute of Science and Technology, Japan, for his technical support. Authors also would like to thank Mr. Kuan Chen Wu at the Graduate School of Materials Science, National Yunlin University of Science and Technology, Taiwan, for his XRD support.

References

1. F. Recart, I. Freire, L. Pérez, R. Lago-Aurrekoetxea, J.C. Jimeno, G. Bueno, *Sol. Energy Mater. Sol. Cells*, 91 (2007) 897.
2. P.N. Vinod, *J. Electron Mater.*, 42 (2013) 2905.
3. M.M. Hilali, S. Sridharan, C. Khadilkar, A. Shaikh, A. Rohatgi, S. Kim, *J. Electron. Mater.,* 35 (2006) 2041.
4. G. Schubert, F. Huster, P. Fath, *Sol. Energy Mater. Sol. Cells,* 90 (2006) 3399.
5. R. Hoenig, A. Kalio, J. Sigwarth, F. Clement, M. Glatthaar, J. Wilde, D. Biro, *Sol. Energy Mater. Sol. Cells*, 106 (2012) 7.
6. J. Bartsch, A. Mondon, C. Schetter, M. Hörteis, SW. Glunz, *35th IEEE Photovoltaic Specialists Conference*, 2010 1299.
7. J. Bartsch, A. Mondon, K. Bayer, C. Schetter, M. Hörteis, SW. Glunz, *J. Electrochem. Soc.*, 157 (2010) H942.
8. A.A. Istratov, E.R. Weber, *Appl. Phys. A: Mater. Sci. Process.*, 66 (1998) 123.
9. S. Flynn, A. Lennon, *Sol. Energ. Mater. Sol. Cells*, 130 (2014) 309.
10. A. Kale, E. Beese, T. Saenz, E. Warren, W. Nemeth, D. Young, A. Marshall, K. Florent, S.K. Kurinec, S. Agarwal, P. Stradins, *43rd IEEE PVSC*, 2016, 2913.
11. A. Kale, W. Nemeth, C.L. Perkins, D. Young, A. Marshall, K. Florent, S.K. Kurinec, P. Stradins, and S. Agarwal, *ACS Appl. Energy Mater.*, 1 (2018) 2841.
12. Q. Huang, K.B. Reuter, Y. Zhu, V.R. Deline, *ECS J. Solid State Sci. Technol.*, 5 (2016) Q24.
13. Y.R. Cheng, W.J. Chen, K. Ohdaira, K. Higashimine, *Int. J. Electrochem. Sci.*, 13 (2018) 11516.
14. Q. Huang, *ECS J. Solid State Sci. Technol.*, 5 (2016) P51.
15. C.H. Hsiao, J.Y. Wu, W.J. Chen, *J. Mater. Sci.: Mater. Electron.*, 30 (2019) 3539.
16. M. Zhou, Y. Zhao, W. Huang, B.M. Wang, G.P. Ru, Y.L. Jiang, R. Liu, X.P. Qu, *Microelectron. Eng.*, 85 (2008) 2028.

© 2020 The Authors. Published by ESG (www.electrochemsci.org). This article is an open access article distributed under the terms and conditions of the Creative Commons Attribution license (http://creativecommons.org/licenses/by/4.0/).